Enhanced photocurrent in crystalline silicon solar cells by hybrid plasmonic antireflection coatings

Narges F. Fahim,[1] Zi Ouyang,[1] Baohua Jia,[1,a)] Yinan Zhang,[1] Zhengrong Shi,[2] and Min Gu[1,a)]
[1]*Centre for Micro-Photonics, Faculty of Engineering and Industrial Sciences, Swinburne University of Technology, PO Box 218, Hawthorn, 3122 Victoria, Australia*
[2]*Suntech Power Holdings Co., Ltd., 9 Xinhua Road, New District, Wuxi, Jiangsu Province 214028, China*

(Received 13 November 2012; accepted 7 December 2012; published online 26 December 2012)

Photocurrent enhancement induced by plasmonic light trapping is of great interest for photovoltaics. We design and demonstrate hybrid plasmonic antireflection coatings as an efficient light trapping strategy for broadband absorption and photocurrent enhancement in crystalline silicon solar cells. Gold nanoparticles of size ranging from 15 to 150 nm are embedded in standard SiN_x antireflection coatings with a thickness of 90 nm. Through optimizing the location of tailored nanoparticles within the SiN_x layer, both light scattering enhancement and near-field light concentration can be harnessed. A maximum increase of 6.3% in photocurrent is achieved for textured multi-crystalline Si solar cells with the optimum configuration. © *2012 American Institute of Physics*.
[http://dx.doi.org/10.1063/1.4773038]

Reflection losses in photovoltaic cells represent a major bottleneck for achieving high conversion efficiency. Thus, antireflection coating (ARC) is one of the most indispensable components in high performance crystalline silicon (Si) solar cells. The most widely adopted method used in the photovoltaic industry is the deposition of a single layer of SiN_x film on the front surface of solar cells by plasma-enhanced chemical vapour deposition (PECVD) to reduce the light reflection at the Si surface and thereby increase the photocurrent of solar cells. The thickness of the SiN_x layer can be controlled so that destructive interference occurs between the reflected light at the air/SiN_x and SiN_x/Si interfaces.[1] However, due to the phase-matching nature of this type of ARC, reflection minimum can only be achieved at a relatively narrow bandwidth of wavelengths determined by the coating thickness. Yet, broadband antireflection, particularly in the near infrared region from 800 to 1200 nm, remains as a challenge with the conventional light trapping approaches.

Surface plasmon resonances in metal nanoparticles (NPs) have been widely recognized to be able to boost the light absorption of solar cells due to the far-field scattering from the metal NPs.[2–12] By controlling the size, shape, and surrounding dielectric environment of the nanoparticles, the resonant plasmonic scattering can be well tuned to match the weak absorption region of silicon, for example, close to its bandgap. Although near-field enhancement (enhanced localized field in the vicinity of the metal NPs) has been reported to be effective for optically thin solar cells,[13–15] limited success[16] has so far been achieved for optically thick, crystalline Si wafer solar cells, which are dominant in the photovoltaic market. The key challenges lie in two aspects. First, in crystalline Si solar cells, it is difficult for the near-field of the NPs to penetrate the SiN_x ARC (several tens of nanometers) due to its fast decaying nature if the NPs are merely placed on top of SiN_x ARC. Second, the strength of the near-field effect is inversely proportional to the particle size. To achieve large near-field enhancement, the particle size needs to be small. However, on the other hand, small particle size means increased detrimental light absorption in the particles. Therefore, the particle size needs to be tailored, based on the balance of the two opposing effects, in order to achieve the maximum silicon absorption enhancement.

In this letter, we propose a concept of hybrid plasmonic antireflection coatings (HPARCs), which combines the advantages of both a standard SiN_x ARC and the plasmonic effect from gold (Au) NPs, to enhance the absorption and thereby the photocurrent in textured multi-crystalline Si solar cells. By embedding the optimized Au NPs inside the SiN_x ARC layer and adjusting the distance between the NPs and the Si photoactive layer, not only the scattering effect but also the near-field enhancement from the plasmonic NPs can be harnessed, which leads to a superior broadband light trapping that outperforms the cells with a standard SiN_x ARC.

A solar cell with HPARCs is represented schematically in Fig. 1(a), where NPs are embedded in a SiN_x layer with an optimized thickness of 90 nm determined from our previous study.[10] The thickness of the SiN_x layer underneath the NPs (t_{under}) is changed from 10 to 90 nm, and the thickness of SiN_x overcoating the NPs (t_{over}) is designed to be $t_{over} = 90\,\text{nm} - t_{under}$ nm. A range of Au NP sizes are studied from 15 to 150 nm, which enable both strong near-field localization and scattering effect. The solar cell samples are standard textured multi-crystalline Si solar cells (Suntech Power Holdings Co., Ltd.) without the SiN_x ARC. Films of SiN_x ARCs underneath the NPs with desired thickness were first deposited onto the solar cells by PECVD reactor (Plasma system 100, Oxford instruments), followed by integrating the NPs into solar cells via dip coating (KSV company, model: DS). Au NPs were synthesized according to the iterative seeding process with some modifications.[10,17,18] Details of the NP synthesis and the integration into solar cells can be found elsewhere.[10] Au NP colloidal solutions of concentrations 6.4×10^{12}, 1.28×10^{11}, 1.87×10^{10}, and 1.36×10^{10} NPs/ml for sizes 15, 60, 110, and

a)Authors to whom correspondence should be addressed. Electronic addresses: bjia@swin.edu.au and mgu@swin.edu.au.

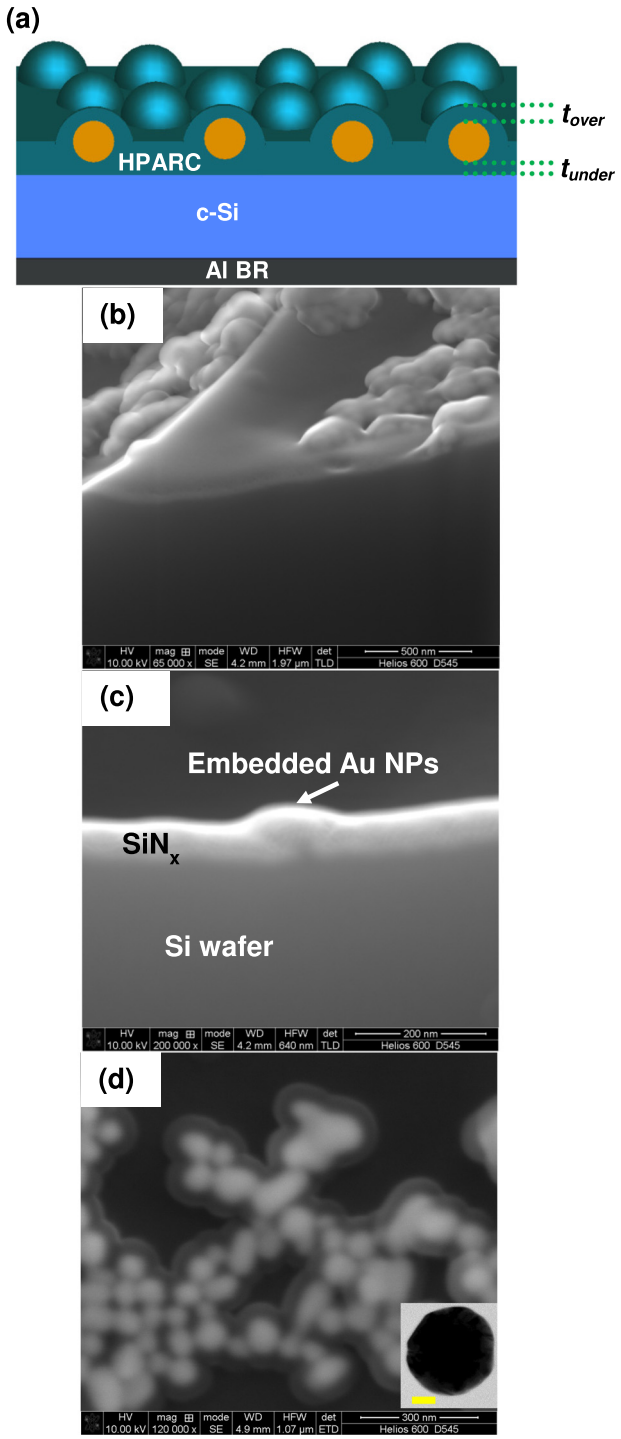

FIG. 1. Schematic diagram of a multi-crystalline Si solar cell incorporating HPARC, where Au NPs are embedded within the SiN_x ARC layer (a). FE-SEM micrographs of cross-sectional view ((b) and (c)) and surface view (d) of embedded Au NPs in SiN_x ARC (10 nm SiN_x: 60 nm Au NP: 80 nm SiN_x). The inset in image (d) is the HR-TEM of 60 nm Au NP without SiN_x coating (the scale bar is 20 nm).

150 nm, respectively, were used. The surface coverage is optimized to be around 12% for all particle sizes. After the NP integration, SiN_x was deposited again with a thickness of (90 nm-t_{under} nm). The thickness and refractive index ($n = 2.03$ at 633 nm) of the SiN_x films were determined by ellipsometry measurements (J. A. Woollam M-2000XI).

Figures 1(b) and 1(c) present the field emission scanning electron microscopy (FE-SEM) micrographs of the embedded Au NPs (60 ± 10 nm in size on average) in the SiN_x ARC layer of configuration (10 nm $SiN_x + 80$ nm SiN_x) on a multi-crystalline Si solar cell. It is evident that Au NPs are overcoated with a film of SiN_x ARC as seen in the surface view (Fig. 1(d)) and cross-sectional view of Figs. 1(b) and 1(c). It is expected that the bumpy topography of the hybrid plasmonic coating, as shown in Fig. 1, will improve the light interaction with the solar cell. Inset of Fig. 1(d) shows the high resolution-transmission electron microscopy (HR-TEM) image of the spherical shape of Au NP.

To systematically evaluate the light trapping provided by the HPARCs, the external quantum efficiency (EQE, PV Measurements, Inc., Model QEX10) measurements were performed for wavelengths ranging from 300 to 1200 nm. The EQE measures the ratio of the photo-generated and collected electrons to the incident photons as a function of the wavelength. The short-circuit current density (J_{sc}) can be directly calculated from the EQE data as following $J_{SC} = q\int EQE(\lambda)S(\lambda)d\lambda$, where q is the electron charge and $S(\lambda)$ is the standard spectral photon density of sunlight at the surface of the earth (Air Mass 1.5 global, AM1.5G). The EQE determined J_{sc} value excludes uncertainties due to the spectral mismatch between the AM1.5G spectrum and the solar simulator. The effects of the HPARCs were determined by comparing the same cell before and after the NP integration. By this way, we ruled out the sample-to-sample uncertainty.

The J_{sc} enhancement estimated from the EQE measurements for solar cells with HPARCs as a function of the NP size and spacing layer thickness (t_{under}) is shown in Fig. 2(a). The peak EQE enhancement is observed at the medium NP size of 60 nm and the minimum spacing layer thickness of 10 nm. The J_{sc} enhancement is closely related to the changes of the NP size and their distance to the Si photoactive layer. To achieve the maximum J_{sc} enhancement, the optimized particle size and the distance need to be identified to understand the optimum cell design and balance the following factors simultaneously: (i) strong coupling of light in the solar cells; (ii) strong scattering of light at the weak-absorbing wavelengths; (iii) strong near-field enhancement in the active layer, and (iv) minimum NP absorption. In terms of particle size selection, the 15 nm NPs are expected to have the largest near-field enhancement[3] due to the highest field localization. But, the overall performance suffers from strong parasitic absorption of these small NPs.[19] Although large NP sizes of 110 nm and 150 nm can effectively scatter the weakly absorbing light at the bandgap, they cannot bring in beneficial near-field enhancement.[20–22] In comparison, the 60 nm NPs possess both reasonable near-field localization and strong scattering matching the peak of the solar spectrum, and therefore shows the largest enhancements among all the investigated NP sizes, as shown in Fig. 2(a).

In Fig. 2(b), we plot the J_{sc} data for the 60 nm NPs as a function of the spacing layer thickness to better analyze the coupling effect of the near-field and scattered light with Si active layer. It is seen from Fig. 2(a) that the photocurrent enhancement increased exponentially with the reduced spacing layer thickness. The coupling efficiencies of the near-field and scattered light are largely determined by the NP distance to the Si photoactive layer. For the case that NPs are on the surface of the 90 nm SiN_x layer, the near-field

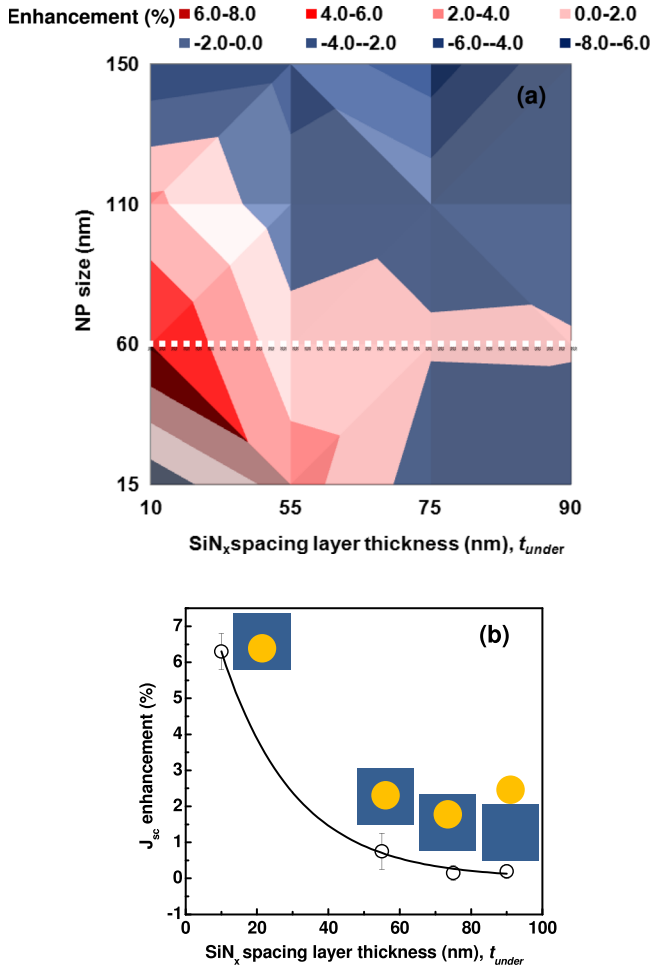

FIG. 2. Enhancement of (a) EQE-determined short-circuit photocurrent density (J_{sc}) of solar cells with HPARCs as a function of the NP size and the SiN_x thickness underneath the NPs (spacing layer), and J_{sc} enhancement (b) as a function of spacing layer thickness for 60 nm NPs. It corresponds to the white dotted line in (a) referring to the highest enhancements. Schematic structures in (b) show the position of Au NPs in the SiN_x ARC layer.

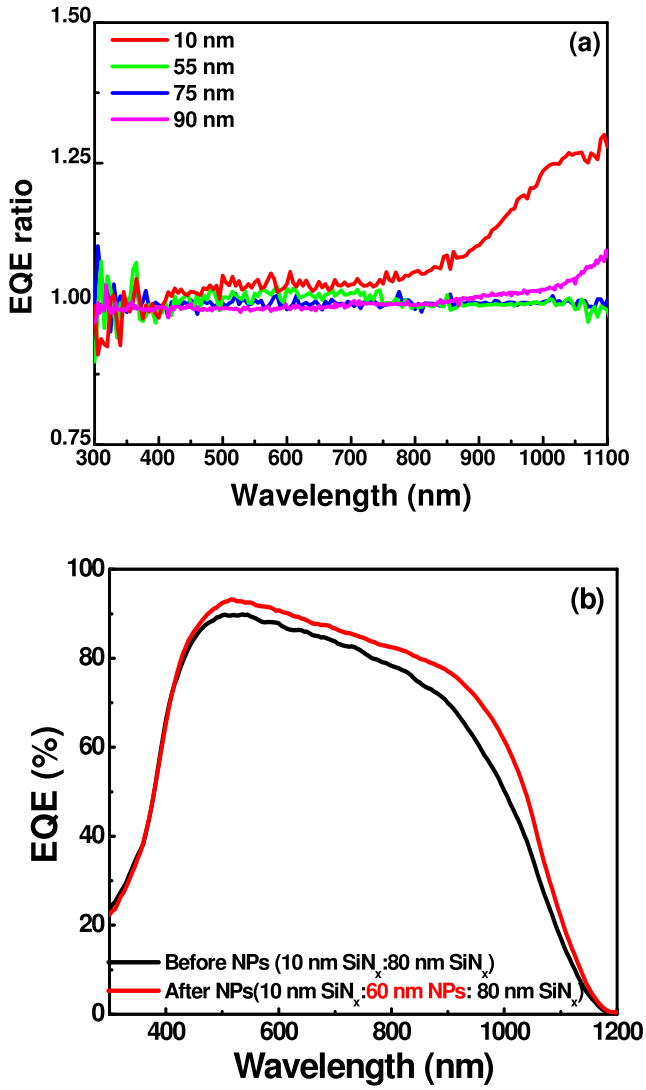

FIG. 3. EQE variation after the integration of NPs normalized to the reference cell. SiN_x spacing layer thicknesses of 10, 55, 75, and 90 nm are shown (a). EQE of the highest enhanced photocurrent corresponding to the structure of 10 nm SiN_x: 60 nm NP: 80 nm SiN_x (b). The EQE of the solar cell with SiN_x ARC only is also presented as reference.

coupling is vanished due to the large distance comparable to the penetration depth of the near-field of NPs. The coupling strength of the scattered light with the Si layer in this case is also weak compared to the embedded case because of the limited angular distribution of the scattered light.[21] Larger enhancement in photocurrent is achieved as the thickness of the spacing layer reduced from 90 nm to 10 nm. This is because the coupling efficiencies of both the near-field and the scattered light increase with reducing spacing layer thickness.[3,9,23] In particular, when the thickness is less than 20 nm, J_{sc} enhancement increases dramatically. It reaches a maximum of 6.3% (absolute value increases from 32.11 to 34.14 mA/cm^2) when the spacing layer thickness is minimum (10 nm). A larger coupling efficiency is expected with further decreasing the spacing layer thickness but it may lead to increased recombination of the solar cells.

To better understand the mechanisms behind the photocurrent enhancement, the EQE enhancement variation (normalized to the same solar cells without NPs) for solar cells incorporating 60 nm NPs at different spacing layer thicknesses is presented in Fig. 3(a). For solar cells incorporating NPs on the top of the SiN_x layer, a broadband enhancement was observed at longer wavelengths from 800 to 1200 nm with a slight reduction at shorter wavelengths in the range from 400 to 750 nm, which results in a small overall enhancement characterized by photocurrent described in Fig. 2. The enhancement in EQE was attributed to the enhanced light trapping due to the strong and broad forward scattering from Au NPs, which manifested an enhancement in photocurrent. Nevertheless, the backscattering and dissipation in Au NPs are the main reasons for reduction of the EQE at shorter wavelengths below the resonance.[24] A modest enhancement can be seen for solar cells incorporate HPARCs of structure configuration (75 nm SiN_x: 60 nm NPs: 15 nm SiN_x).

By continuously decreasing the thickness of the spacing layer between the NPs and Si photoactive layer to 55 nm, the EQE was enhanced at shorter wavelengths from 400 to 750 nm with almost no change across the long wavelengths. By further reducing the spacing layer to 10 nm, the EQE was significantly enhanced over the entire solar spectrum from 400 to 1200 nm with the maximum enhancement of 25% at the wavelength of 1100 nm. The EQE spectra for the solar cell with the optimized HPARC (10 nm SiN_x: 60 nm NPs:

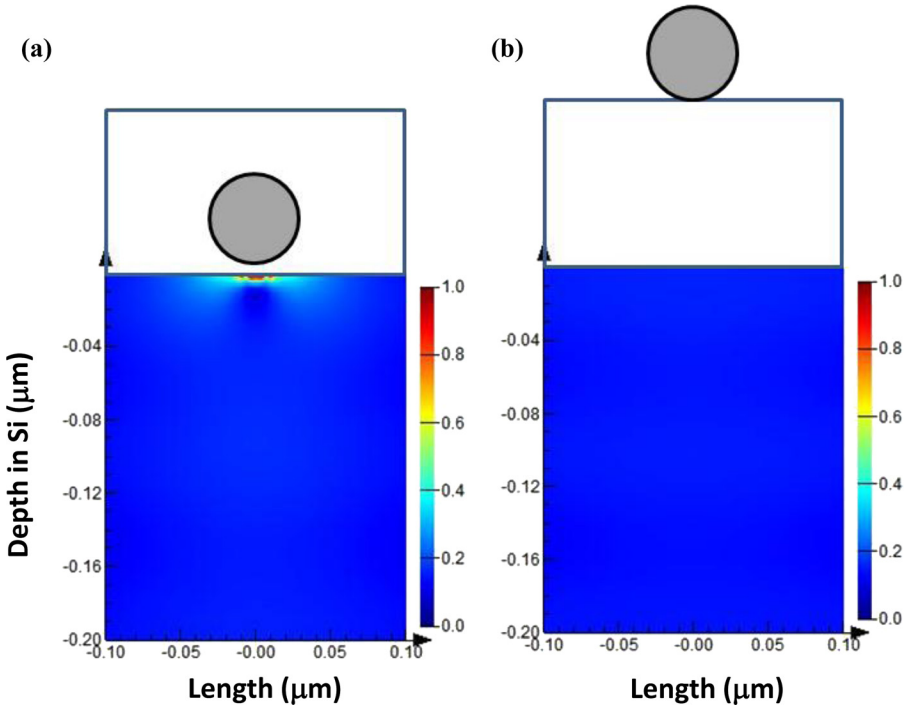

FIG. 4. Field intensity profiles in Si with an Au nanoparticle (a) embedded in the SiN_x ARC of the optimized configuration (10 nm SiN_x: 60 nm Au NP: 80 nm SiN_x) and (b) on the top surface of 90 nm-thick SiN_x ARC. The incoming wavelengths were selected $\lambda = 700$ nm, around the plasmonic resonance.

80 nm SiN_x) are depicted in Fig. 3(b) in comparison to the reference cell without NPs. The EQE has been enhanced over broad wavelengths from 430 to 1200 nm for the cell incorporating the optimum configuration of HPARCs. More interestingly, no EQE reduction was observed even for the short wavelengths with the optimized HPARCs. Reducing the spacing between the NPs and Si layer to few tens of nanometers enables an effective overlap between the active layer and the concentrated near-field excited by the NPs, enhancing light absorption locally on the active layer surface.[12] The increased absorption is manifested as an increase in the measured photocurrent as shown in Fig. 3.

Figures 4(a) and 4(b) show FDTD simulated (Lumerical Software)[8,25] field intensity profiles under 700 nm light illumination in Si with Au nanoparticle embedded in SiN_x ARC of configuration (10 nm SiN_x: 60 nm Au NP: 80 nm SiN_x) and on the top surface of 90 nm-thick SiN_x ARC, respectively. It can be seen that there exists a strong near field in the close vicinity of the 60 nm NPs. However, due to the difference in the thickness and thus the refractive index of the surrounding environment, the light concentration intensity in the 10 nm spacing layer configuration is much stronger than the configuration of 90 nm spacer. The calculated penetration depths of the near-fields in both configurations are less than 20 nm, which inevitably lead to a strong coupling of the field in the 10 nm spacing layer configuration in comparison to the 90 nm spacing layer configuration, in which no obvious enhancement can be detected in the silicon active layer, as shown in Fig. 4.

To sum up, we have demonstrated a promising design strategy of hybrid plasmonic antireflection coatings to enhance the photocurrent in textured multi-crystalline Si solar cells. Through optimizing the plasmonic NP size and tailoring their embedded location in the standard SiN_x ARC, both effective scattering and near-field enhancement can be harnessed. Consequently, the optimized absorption enhancement covering almost the entire Si absorption band has been achieved, leading to a significant increase in the photocurrent by 6.3%. This study clearly shows that careful design of the hybrid plasmonic antireflection coatings can result in significant photocurrent enhancement in the optically thick, crystalline Si wafer solar cells.

The authors acknowledge the financial support from the Victorian Government to establish the Victoria-Suntech Advanced Solar Facility (VSASF) under the Victoria Science Agenda (VSA) scheme. Baohua Jia thanks the Victorian Government for the support through the Victorian Fellowship.

[1]H. K. Raut, V. A. Ganesh, A. S. Nair, and S. Ramakrishna, Energy Environ. Sci. **4**, 3779 (2011).
[2]P. Spinelli, M. Hebbink, R. de Waele, L. Black, F. Lenzmann, and A. Polman, Nano Lett. **11**, 1760 (2011)
[3]H. A. Atwater and A. Polman, Nature Mater. **9**, 205 (2010).
[4]S. Pillai, K. R. Catchpole, T. Trupke, and M. A. Green, J. Appl. Phys. **101**, 093105 (2007).
[5]P. Matheu, S. H. Lim, D. Derkacs, C. McPheeters, and E. T. Yu, Appl. Phys. Lett. **93**, 113108 (2008).
[6]H. R. Stuart and D. G. Hall, Appl. Phys. Lett. **69**, 2327 (1996).
[7]N. F. Fahim, B. Jia, Z. Shi, and M. Gu, Opt. Express **20**, A694 (2012).
[8]Y. Zhang, Z. Ouyang, N. Stokes, B. Jia, Z. Shi, and M. Gu, Appl. Phys. Lett. **100**, 151101 (2012).
[9]K. R. Catchpole and A. Polman, Appl. Phys. Lett. **93**, 191113 (2008).
[10]N. F. Fahim, Z. Ouyang, Y. Zhang, B. Jia, Z. Shi, and M. Gu, Opt. Mater. Express **2**, 190 (2012).
[11]X. Chen, B. Jia, J. K. Saha, B. Cai, N. Stokes, Q. Qiao, Y. Wang, Z. Shi, and M. Gu, Nano Lett. **12**, 2187 (2012).
[12]M. Gu, Z. Ouyang, B. Jia, N. Stokes, X. Chen, N. Fahim, X. Li, M. J. Ventura, and Z. Shi, "Nanoplasmonics: A frontier of photovoltaic solar cells," Nanophotonics (in press).
[13]A. J. Morfa, K. L. Rowlen, T. H. Reilly, M. J. Romero, and J. Van de Lagemaat, Appl. Phys. Lett. **92**, 013504 (2008).
[14]C. Hägglund, M. Zäch, and B. Kasemo, Appl. Phys. Lett. **92**, 013113 (2008).
[15]R. B. Konda, R. Mundle, H. Mustafa, O. Bamiduro, A. K. Pradhan, U. N. Roy, Y. Cui, and A. Burger, Appl. Phys. Lett. **91**, 191111 (2007).
[16]D. M. Schaadt, B. Feng, and E. T. Yu, Appl. Phys. Lett. **86**, 063106 (2005).
[17]G. Frens, Nat. Phys. Sci. **241**, 20 (1973).

[18]K. R. Brown, D. G. Walter, and M. J. Natan, Chem. Mater. **12**, 306 (2000).
[19]S. Pillai and M. A. Green, Sol. Energy Mater. Sol. Cells **94**, 1481 (2010).
[20]F. J. Beck, E. Verhagen, S. Mokkapati, A. Polman, and K. R. Catchpole, Opt. Express **19**, A146 (2011).
[21]I. Diukman and M. Orenstein, Sol. Energy Mater. Sol. Cells **95**, 2628 (2011).
[22]T. L. Temple and D. M. Bagnall, "Broadband scattering of the solar spectrum by spherical metal nanoparticles," Prog. Photovoltaics.
[23]K. R. Catchpole and A. Polman, Opt. Express **16**, 21793 (2008).
[24]C. Hägglund, M. Zäch, G. Petersson, and B. Kasemo, Appl. Phys. Lett. **92**, 053110 (2008).
[25]FDTD solutions (Lumerical, Toronto, Canada).